Vorticity structure and polarization of Λ - hyperons in Au-Au collisions

A.V. Zinchenko, O.V. Teryaev, M.I. Baznat

Yaroslavl State University, Russia; JINR, Dubna, Russia

5th International Conference on Particle Physics and Astrophysics (ICPPA-2020) MEPhI, Moscow, Russia, 7 October 2020

Outline

1. Introduction
2. PHSD model
3. Vorticity structure
4. Helicity separation
5. Polarization
6. Summary

Introduction

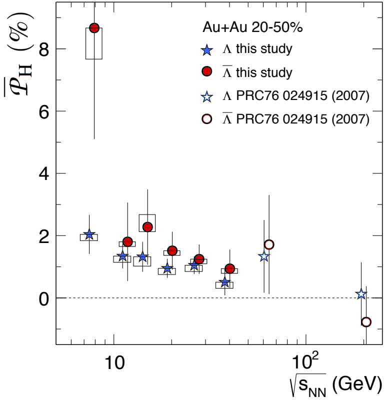

fig: 1. The average polarization $\overline{P}_{\mathrm{H}}$ (where $\mathrm{H} = \Lambda$ or $\bar{\Lambda}$) from 20-50% central Au+Au collisions is plotted as a function of collision energy(STAR data (Nature 548 (2017) 62-65)).

PHSD model

The Parton-Hadron-String Dynamics (PHSD) (arXiv:0808.0022 [hep-ph]) is a microscopic off-shell transport approach that consistently describes the full evolution of a relativistic heavy-ion collision from the initial hard scatterings and string formation through the dynamical deconfinement phase transition to the quark-gluon plasma as well as hadronization and to the subsequent interactions in the hadronic phase.

To calculate the vorticity field, we need to know the velocity field $\vec{v}(x)$. In relativistic system, the definition of the velocity is not unique. We define several types of velocity field, $\vec{v}_1$, $\vec{v}_2$ and $\vec{v}_3$:

$$v_1^a(x) = \frac{\sum_i p_i^a F(x, x_i)}{\sum_i p_i^0 F(x, x_i)}, \tag{1}$$

$$v_2^a(x) = \frac{1}{\sum_i F(x, x_i)} \sum_i \frac{p_i^a}{p_i^0} F(x, x_i), \tag{2}$$

$$v_3^a(x) = \frac{\sum_i p_i^a F(x, x_i)}{\sum_i [p_i^0 + (p_i^a)^2/p_i^0] F(x, x_i)}, \tag{3}$$

where $a = 1, 2, 3$ is the spatial indices, p_i^a and p_i^0 are the momentum and energy of the i-th particle, and the summation is over all the particles. We will use the first one.

Vorticity structure

There are several definitions of vorticity. We will use the non-relativistic and relativistic kinetic vorticity:

$$\varpi_{\mu\nu} = \frac{1}{2}(\partial_\nu v_\mu - \partial_\mu v_\nu)\,, \quad \omega_{\mu\nu} = \frac{1}{2}(\partial_\nu u_\mu - \partial_\mu u_\nu)\,, \qquad (4)$$

where u_ν is a relativistic four-vector of the velocity field.

$$u_\nu(t,\vec{x}) = \gamma(1,\vec{v}(t,\vec{x}))\,, \quad \gamma(t,\vec{x}) = \frac{1}{\sqrt{1-\vec{v}^{\,2}(t,\vec{x})}}\,. \qquad (5)$$

In the case of relativistic vorticity, γ-factor has a significant influence on the fireball boundaries, strengthening vorticity value (fig. 2).

Vorticity structure

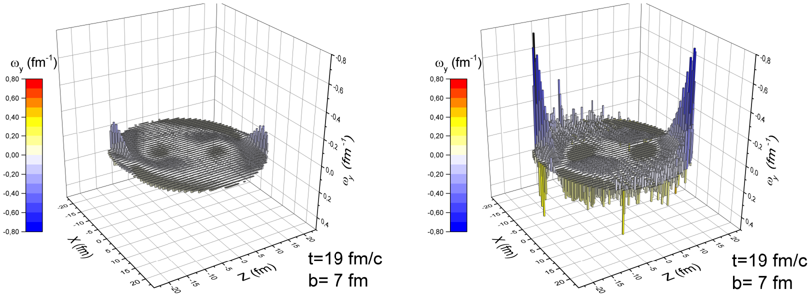

a) b)

fig: 2. Y-component of vorticity in reaction plane XZ($y = 0$) in the case of the classical definition -a) and relativistic -b) at energy $\sqrt{s} = 7.7$ GeV.

It takes the largest value on the boundaries of fireball and spectators, and it has the same sign on both boundaries, which together gives a non-zero ω_y vorticity in the XZ plane(Fig. 2).

Vorticity structure

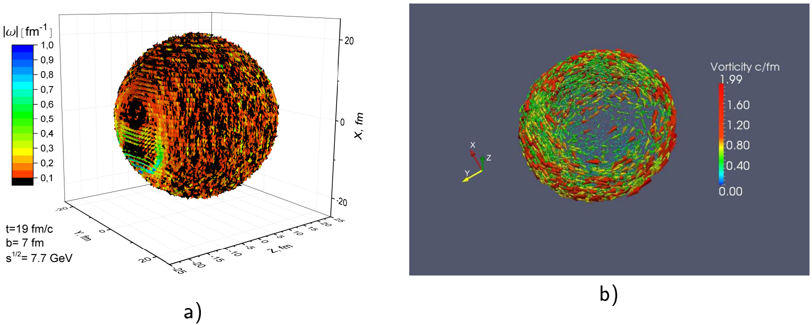

fig: 3. Vortex sheet in the PHSD model a) and QGSM b).

Since 15 fm/c the so-called vortex sheet begins to form on the boundary of the fireball at energy $\sqrt{s} = 7.7$ GeV. It is observed both in the QGSM and in the PHSD -model(see fig. 3.3). In the PHSD model, the structure has a significant vorticity on the border of participants and spectators(Fig. 2 b), Fig. 3).

Vorticity structure

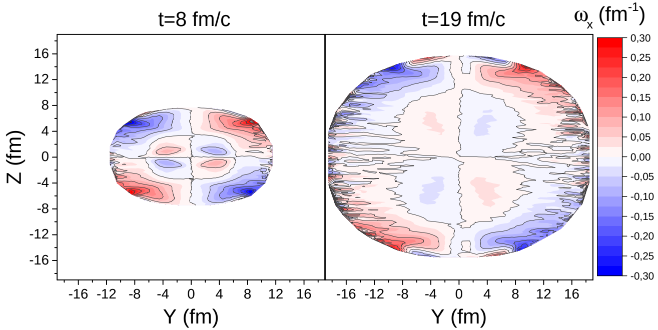

fig: 4.Quadrupole structure of relativistic vorticity ω_x in Au+Au ($\sqrt{s} = 7.7$ GeV), $x = 0$, $b = 7$ fm.

We can see the presence of a vortex sheet in the perpendicular plane ZY (see Fig. 4 b). An increase in the x-component of vorticity is observed around the boundary of fireball and there are maximums at the boundary with spectators, as in plane XZ. But we also see a mirror quadrupole structure with an internal part having an opposite sign with respect to the corresponding external region.

Vorticity structure

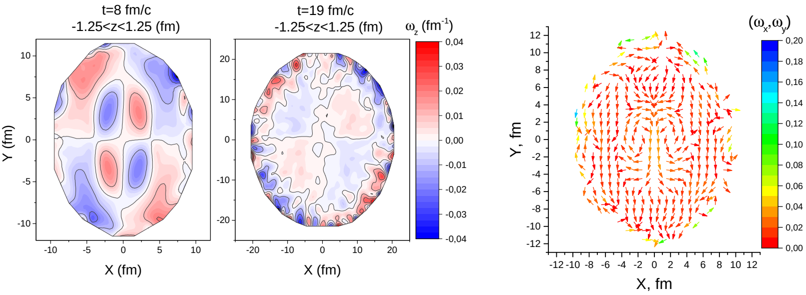

a) b)

fig: 5. a) Quadrupole structure of relativistic vorticity ω_z in Au+Au ($\sqrt{s} = 7.7$ GeV), at different time. Averaging was performed in the 2.5 fm range in the layer $z = 0$. b) Structure of the transverse vorticity $\vec{\omega}_\perp = (\omega_x, \omega_y)$ in Au+Au ($\sqrt{s} = 7.7$ GeV, $t = 8$ fm/c, $b = 7$ fm), in the center of the fireball $z = 0$.

Vorticity structure

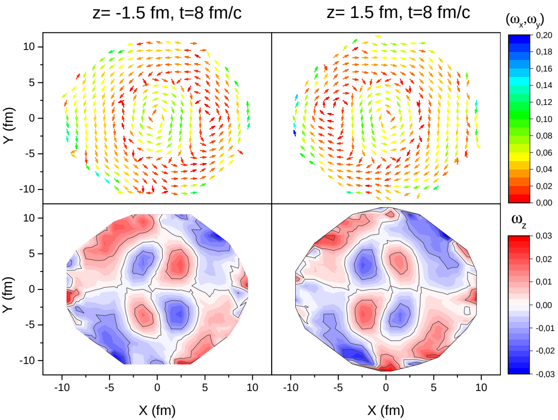

fig: 6. Quadrupole structure of relativistic vorticity ω_z in Au+Au ($\sqrt{s} = 7.7$ GeV) in the bottom line and corresponding structure of the transverse vorticity $\vec{\omega}_\perp = (\omega_x, \omega_y)$ in the same time and layer of z.

Vorticity structure

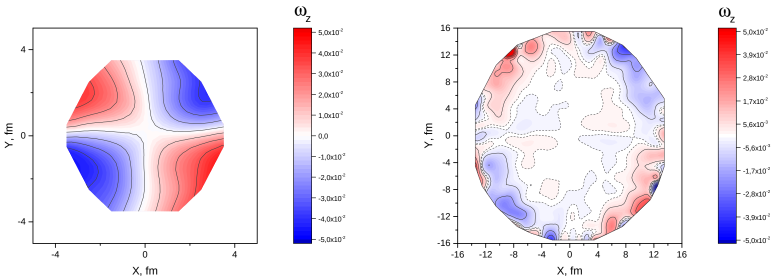

a) b)

fig: 7. Quadrupole structure of relativistic vorticity ω_z in Au+Au ($\sqrt{s} = 7.7$ GeV, $b = 8$ fm), at different time($t = 9.5$ fm/c - left one, $t = 13$ fm/c - right one) without P-P potential. Averaging was performed in the 5 fm range in the layer $z = 0$.

Vorticity structure

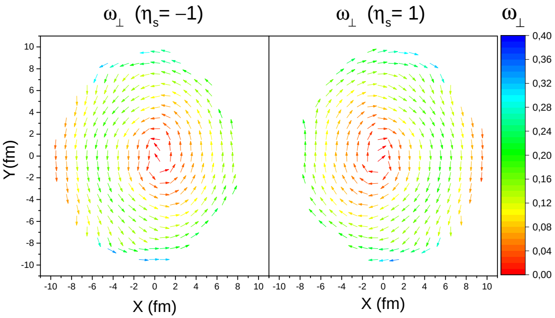

fig: 8. The distribution of the transverse vorticity $\vec{\omega}_\perp = (\omega_x, \omega_y)$ in the transverse plane at longitudinal position $\eta_s = -1$ (left) and $\eta_s = 1$ (right) ($\eta_s = 1/2\, ln\,[(t+z)\,/\,(t-z)]$) at time $t = 9.5$ fm/c, b= 5 fm ($\sqrt{s} = 7.7$ GeV). It is consistent with the work (arXiv:1810.00151 [nucl-th]), where similar structures for thermal vorticity are obtained.

Vorticity structure

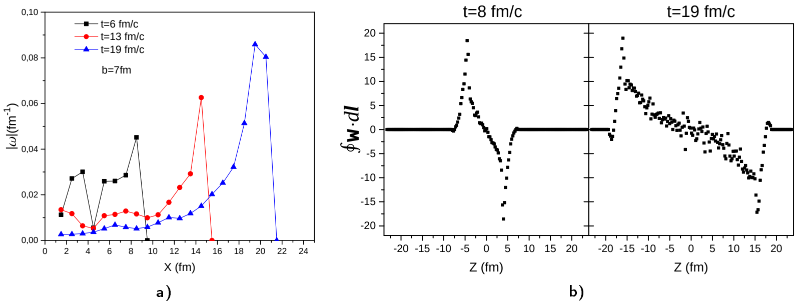

fig: 9. a) Dependence of the vorticity modulus on the fireball radius at different times ($b = 7$ fm, $z = 0$, $\sqrt{s} = 7.7$ GeV). b) Vorticity field circulation in the XY plane as a function of z in different time.

Having summed up all the previous figures, we conclude that the vorticity field has a spherical elongated shape, at poles (along Z) of which it is maximum, and one half of this sphere rotates in one direction and reverse in the other, having the opposite rotation in the center. But the total rotation tends to zero when approaching $z = 0$. We can see this by taking the circulation of vorticity vector at various points z in XY-plane (Fig. 8 b). At the same time, the vorticity modulus at z = 0 grows towards the boundary (except at times of order 6 fm/c, there is a significant modulus of vorticity inside the fireball) of the fireball and increases with time. This means that near $z = 0$ there is no distinguished direction of rotation of vorticity field, and when moving away from zero, two opposite rotations are formed.

Helicity separation

Helicity contributes directly to the polarization of hyperons in so-called axial vortical effect approach. The effect is proportional to vorticity and helicity of the strong interacting medium, and, in particular, to helicity separation effect discovered (arXiv:1301.7003 [nucl-th]) in the kinetic Quark-Gluon-String Model(QGSM) and PHSD model(Fig. 9).

$$< \Pi_0^\Lambda > = < \frac{m_\Lambda}{N_\Lambda\, p_y} > \frac{N_c}{2\pi^2} \int d^3x\, \mu_s^2(x) \gamma^2 \epsilon^{ijk} \upsilon_i \partial_j \upsilon_k, \tag{6}$$

where the hydrodynamic helicity is contained within the integral $H \equiv \int d^3x (\vec{\upsilon} \cdot \vec{\omega})$. Helicity separation effect receives the significant contribution $\sim \vec{\upsilon}_y \vec{\omega}_y$ from the transverse component of velocity and vorticity. It is easily explained by the same signs of transverse vorticities in the "upper"and "lower"(w.r.t. reaction plane) half-spaces, combined with the opposite signs of velocities. Even larger contribution of longitudinal components of velocity and vorticity $\sim \vec{\upsilon}_z \vec{\omega}_z$ implies the appearance of the "quadrupole"structure of longitudinal vorticity.

Helicity separation

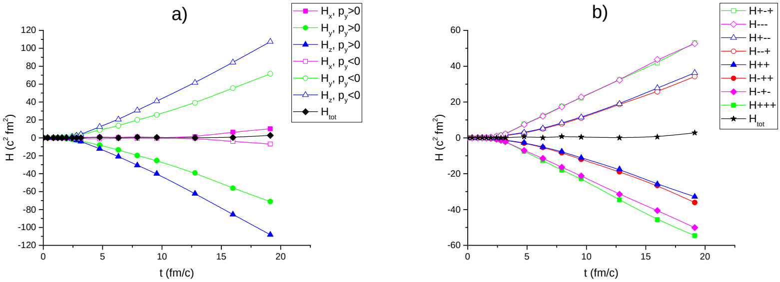

fig: 10. a) Helicity H (fm^2c^2) separation relative to y-component of momentum (impact parameter $b = 7$ fm, $\sqrt{s} = 7.7$ GeV). b) Helicity H (fm^2c^2) separation relative to spatial octants (impact parameter $b = 7$ fm, $\sqrt{s} = 7.7$ GeV), "+++"means that integration was performed in octant $x > 0$, $y > 0$, $z > 0$ and "$---$ $x < 0$, $y < 0$, $z < 0$ respectively.

Polarization

The polarization of λ-hyperons is calculated in the framework of approach exploring local equilibrium thermodynamics(arXiv:1403.6265 [hep-th]) and in the axial vortical effect approach with $b = 7$ fm, energy $\sqrt{s} = 7.7$ GeV and rapidity $|y| < 1$ ($y = 1/2 \log((E + p_z)/(E - p_z))$). In Thermodynamics approach spin vector $\vec{S}^*$ averaged over the $\vec{p}_\Lambda$ direction is determined by

$$\langle \vec{S}^*_\Lambda \rangle_{\vec{n}_p} = \frac{(1 - n_\Lambda)}{4M_\Lambda} \left(E_\Lambda + \frac{1}{3} \frac{\vec{p}^{\,2}_\Lambda}{E_\Lambda + m_\Lambda} \right) \mathrm{rot}\vec{\beta}\,. \tag{7}$$

where $\vec{\beta}$ - thermodynamical velocity(v/T). The results are $\Pi_0^\lambda = 0.7\%$ for thermodynamics one and $\Pi_0^\lambda = 8\%$ for anomaly approach, which is very sensitive to chemical potential. We see an order of magnitude difference, which can be related firstly in the choice of determining velocity, and secondly in the sensitivity of thermodynamic quantities.

Polarization

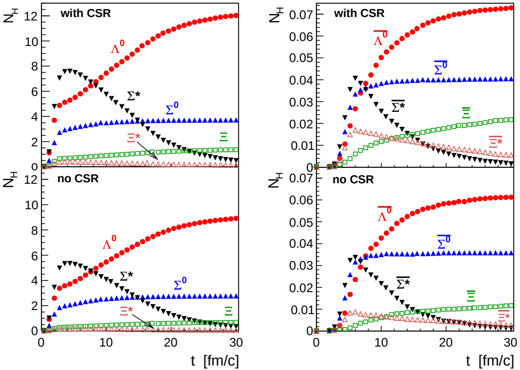

fig: 11.Average numbers of strange particles (left panel) and anti-particles (right panel) as functions of collision time for Au+Au ($\sqrt{s} = 7.7$ GeV) with the impact parameter $b = 7.5$ fm. The upper panels correspond to the results calculated with and the bottom ones without the chiral symmetry restoration effect.(arXiv:1801.07610v1)

Summary

1. Simulations of Au-Au collisions in the PHSD model are performed. The structure of vorticity field of a collisional medium is studied.
2. Helicity separation effect is discovered.
3. The value of Λ - hyperons polarization in various approaches is obtained.